

Electric field control of magnetic properties and magneto-transport in composite multiferroics

O. G. Udalov

Department of Physics and Astronomy, California State University Northridge,
Northridge, CA 91330, USA

Institute for Physics of Microstructures, Russian Academy of Science, Nizhny
Novgorod, 603950, Russia

E-mail: oleg.udalov@csun.edu

N. M. Chtchelkatchev

Department of Physics and Astronomy, California State University Northridge,
Northridge, CA 91330, USA

L.D. Landau Institute for Theoretical Physics, Russian Academy of Sciences, 117940
Moscow, Russia

Department of Theoretical Physics, Moscow Institute of Physics and Technology,
141700 Moscow, Russia

I. S. Beloborodov

Department of Physics and Astronomy, California State University Northridge,
Northridge, CA 91330, USA

PACS numbers: 75.85.+t, 75.30.-m, 75.47.-m, 77.80.-e

Abstract. We study magnetic state and electron transport properties of composite multiferroic system consisting of a granular ferromagnetic thin film placed above the ferroelectric substrate. Ferroelectricity and magnetism in this case are coupled by the long-range Coulomb interaction. We show that magnetic state and magneto-transport strongly depend on temperature, external electric field, and electric polarization of the substrate. Ferromagnetic order exists at finite temperature range around ferroelectric Curie point. Outside the region the film is in the superparamagnetic state. We demonstrate that magnetic phase transition can be driven by an electric field and magneto-resistance effect has two maxima associated with two magnetic phase transitions appearing in the vicinity of the ferroelectric phase transition. We show that positions of these maxima can be shifted by the external electric field and that the magnitude of the magneto-resistance effect depends on the mutual orientation of external electric field and polarization of the substrate.

1. Introduction

Control of magnetic state and magneto-transport properties by an electric field is one of the main challenges in condensed matter physics and materials science these days [1, 2, 3, 4, 5, 6, 7, 8]. There are several known mechanisms of magneto-electric coupling: i) electric field influence on a surface magnetic properties of magnetic films [9, 10, 11], ii) spin-orbit interaction of electrons in a single crystal multiferroics [12, 13], and iii) strain mediated coupling of ferroelectrics (FE) and ferromagnets (FM) [14, 15, 16]. Also the magneto-electric coupling appearing due to the control of the exchange bias in the multiferroic/ferromagnet interface is actively discussed these days. [17, 18, 19] The magnetoresistance can be controlled by electric field using two effects: i) electron spin accumulation in the vicinity of FE boundary due to screening effects [20, 21], and ii) electron spin-orbit interaction [22, 23].

Recently, a new mechanism of magneto-electric coupling was proposed in composite multiferroics — materials consisting of ferromagnetic grains embedded in a ferroelectric matrix [24]. This mechanism is based on the interplay of Coulomb blockade, ferroelectricity, and exchange interaction. It was shown that the intergrain exchange interaction has a pronounced peak due to strong temperature dependence of dielectric susceptibility of FE component of composite multiferroic in the vicinity of the paraelectric-ferroelectric phase transition. This leads to the unusual magnetic phase diagram of composite multiferroics with FM state appearing in a finite temperature range around FE Curie temperature and superparamagnetic state existing outside this region.

Here we focus on the spatially separated ferroelectric and the granular ferromagnetic films, see figure 1. The long range Coulomb interaction establishes the coupling between the ferroelectric and ferromagnetic degrees of freedom. We show that in contrast to the magneto-electric coupling arising due to the spin-orbit interaction the coupling in composite multiferroics is non-linear and is similar to the strain mediated magneto-electric effect.

The dielectric permittivity of FE can be controlled not only by temperature but also using an external electric field [25, 26, 27]. This opens the opportunity to control the magnetic state of the system proximity coupled to FE using the electric field. In this manuscript we predict that electric field can control the magnetic state of granular ferromagnetic thin film placed above the FE substrate. In particular, we show that electric field can induce the magnetic phase transition in the system. We calculate the magneto-resistance effect and show that it can be controlled by an external electric field and it depends on the electric polarization of FE component of the system.

The paper is organized as follows. In section 2 we introduce the model and discuss important energy scales. In sections 3, 4, and 5 we study the influence of FE substrate on the intergrain exchange coupling. We investigate magnetic properties of the system in sections 6 and show that using electric field one can control the magnetization and magnetic susceptibility. Section 7 describes the magneto-electric coupling in composite

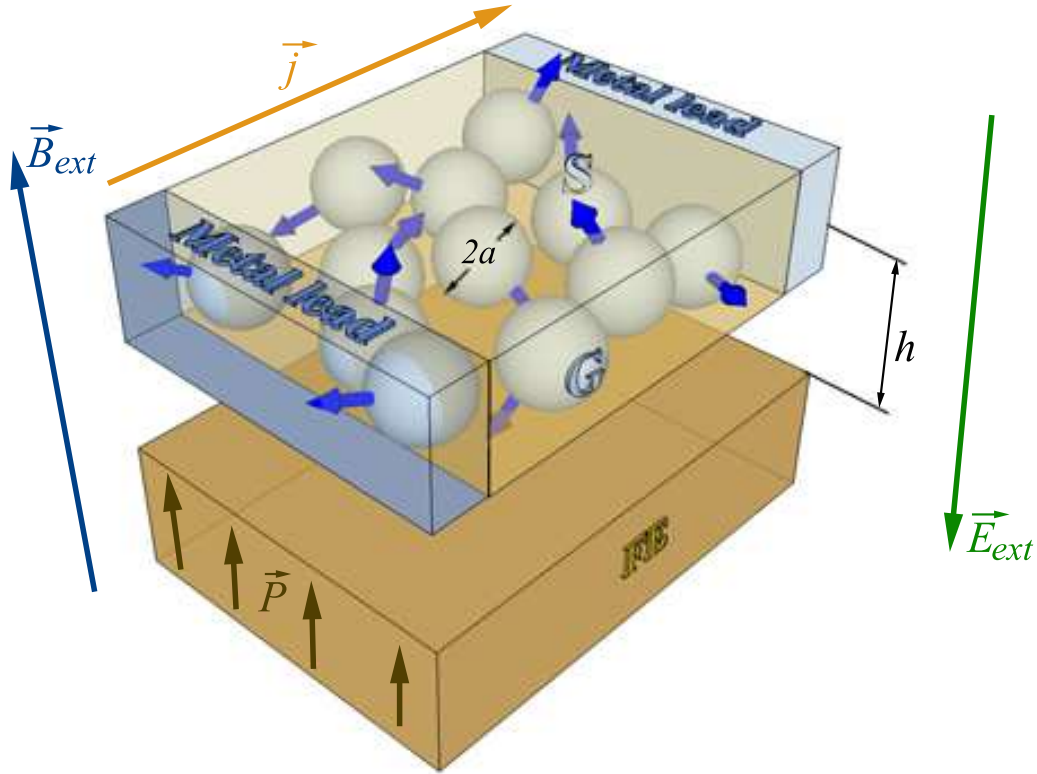


Figure 1. (Color online) Sketch of composite multiferroic system consisting of a granular ferromagnetic film placed above the ferroelectric substrate (FE) at distance h . Granular ferromagnet consists of ferromagnetic metallic grains (G) of average size $2a$ embedded in an insulating matrix. Each grain is in the ferromagnetic state with average spin S . Ferroelectric is polarized (\vec{P}) perpendicular to its surface. The system is placed into magnetic (\vec{B}_{ext}) and electric (\vec{E}_{ext}) external fields. The electric field is perpendicular to the granular film and does not produce a charge current. Small voltage is applied between the leads leading to the electric current \vec{j} .

multiferroics using phenomenological theory. Finally, we study the magneto-resistance (MR) effect as a function of temperature and electric field.

2. The model

We study magnetic and transport properties of the system consisting of magnetic grains embedded in an insulating matrix with FE film (substrate) located in the vicinity of the magnetic granular film, figure 1. The granular film has the thickness d and is located above the FE substrate at distance h , such that $d < h$. The space between the granular film and the FE substrate is filled with an insulator which is used in granular film. A similar insulator is located above the granular film. The magnetic grains have average radius a and the intergrain distance is r_g . For simplicity we neglect the distribution of grain sizes and the intergrain distance distribution inevitably appearing

in granular materials. These effects does not play any crucial role for weak magneto-dipole interaction and anisotropy in comparison with the intergrain interaction.

The magnetic granular film is characterized by several energy scales: 1) the magneto-dipole interaction of grains E_{md} [28, 29], 2) the magnetic Curie temperature of the material of which grains are made T_{C}^{FM} , 3) the energy of magnetic anisotropy E_{a} of a single granule which determines the blocking temperature T_{b} ($T_{\text{b}} \approx E_{\text{a}}$) at which the fluctuations of grain magnetic moments are suppressed by the anisotropy, [30] and 4) the intergrain exchange coupling J and the related ordering temperature T_{m} [31, 32].

For temperatures $T < T_{\text{C}}^{\text{FM}}$ each grain has a finite magnetic moment, typically much larger than $\hbar/2$. For small grains we can neglect the anisotropy energy for temperatures $T > T_{\text{b}}$. We can also neglect the magneto-dipole interaction for temperatures $T \gg E_{\text{md}}$. We assume that magnetic state of the system is defined by the exchange interaction. The influence of granular film thickness on the properties of the system is discussed in Appendix Appendix B.

The granular film is characterized by the charging (or Coulomb) energy $E_{\text{c}} = e^2/(a\epsilon)$, which is the electrostatic energy of a single excess electron placed on a grain [33, 34]. We assume that $E_{\text{c}} \gg T$. In this case the system has an activation conductivity.

The FE substrate is characterized by the polarization \mathbf{P} , which is perpendicular to the substrate surface. The system is placed into external electric \mathbf{E}_{ext} and magnetic \mathbf{B}_{ext} fields. A small voltage is applied along the granular film leading to the electric current \mathbf{j} .

We note that external electric field can be created by applying voltage between some bottom electrode (below the FE layer) and the granular film. Since the granular film has a finite conductivity, the electric potential will be uniformly spread between all grains. Thus, under applied voltage each grain will have some excess charge. [35] This excess charge creates (together with the bottom electrode) a homogeneous electric field governing the FE layer. In addition, there is an inhomogeneous part of the electric field generated by grains. This inhomogeneous part is responsible for ME coupling.

3. Coulomb gap

The important parameter characterizing the properties of granular film is the charging (or Coulomb) energy E_{c} . It controls the electron transport [33, 34], and the exchange coupling between different grains in granular systems [24]. This energy depends on the dielectric permittivity of the space surrounding the grain. Ferroelectrics have tunable dielectric constant. Thus, placing FE in the vicinity of a grain we can control the charging energy.

Considered system consists of several layers with different electric properties. The insulating matrix above and below the granular film has the dielectric permittivity ϵ_{I} . The granular film can be treated using the effective medium approach as an insulator with effective dielectric permittivity ϵ_{G} . We assume that both ϵ_{I} and ϵ_{G} are isotropic and

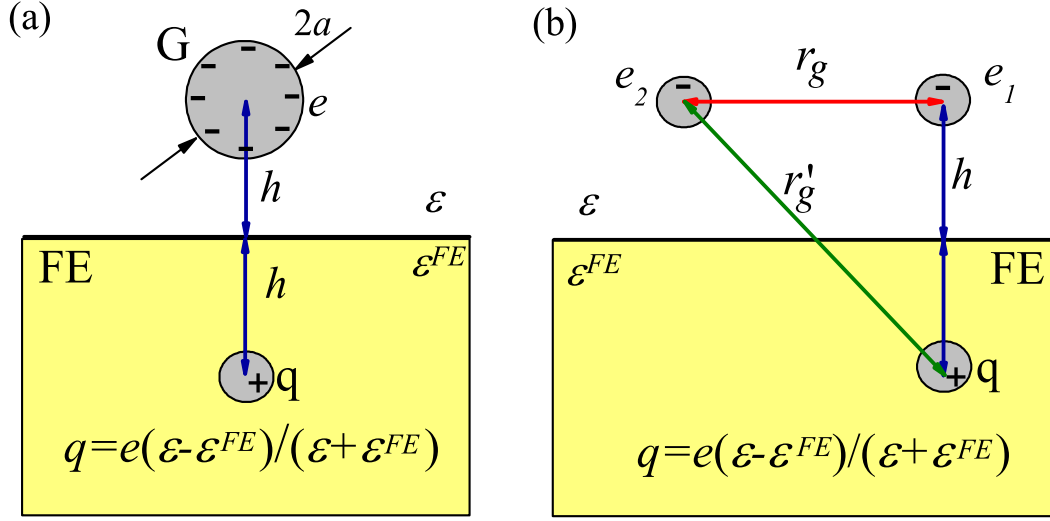


Figure 2. (Color online) (a) Grain (G) with a single excess charge e above the FE substrate (FE). Charge image q appears inside the FE substrate. Interaction with charge q reduces the grain Coulomb energy E_c . (b) Two electrons at distance h above the FE substrate. The distance between electrons is r_g , the distance between the left electron and the charge image q of the right electron is r'_g . Interaction of left electron with image q reduces electrons Coulomb interaction U_c . ϵ and ϵ^{FE} are the dielectric constants of the medium above the FE substrate and the FE substrate, respectively.

do not depend on the external electric field. The dielectric permittivity of the FE layer is anisotropic and depends on the external field. The charging energy of a metallic sphere placed in such a layered structure can be found numerically, Appendix Appendix C. Here we use a simplified model which has an analytical solution. Appendix Appendix C shows that numerical calculations for more complicated model are in a good agreement with analytical result obtained in this section.

Consider a metal sphere with radius a placed above the FE at distance h , $a < h$, see figure 2(a). The sphere is charged with the charge e . The external electric field \mathbf{E}_{ext} is applied to the system in the direction perpendicular to the FE surface (the z -axis), $\mathbf{E}_{\text{ext}} = E_{\text{ext}} \mathbf{z}_0$.

The FE substrate is characterized by the position dependent electric polarization $\mathbf{P}(\mathbf{r}) = \mathbf{P}(\mathbf{E}(\mathbf{r}))$, where \mathbf{r} is the position vector. The electric field $\mathbf{E}(\mathbf{r})$ consists of the spatially homogeneous external field E_{ext} and the inhomogeneous field created by the charged sphere $\mathbf{E}_{\text{el}}(\mathbf{r})$. For simplicity we assume that $E_{\text{ext}} \gg |\mathbf{E}_{\text{el}}|$, and the material relation for FE substrate takes the form $\mathbf{P}(\mathbf{E}) \approx \mathbf{P}_0(E_{\text{ext}}) + (\mathbf{E}_{\text{el}} \cdot \partial_{E_i}) \mathbf{P}_0$. This expansion is valid for electric field less than the FE switching field E_s .[‡] Polarization \mathbf{P}_0 is co-directed with external electric field, $\mathbf{P}_0 = P_0 \mathbf{z}_0$. The partial derivative defines the dielectric susceptibility tensor of the FE-substrate $\hat{\chi}^{FE} = \partial_{E_i} \mathbf{P}_0$. We assume that

[‡] If electron is placed at 10 nm above the FE substrate its electrical field is $E_{\text{el}} \approx 0.1$ MV/cm, while the FE switching field, for example for P(VDF/TrFE) FE, is $E_s \approx 1$, thus $E_{\text{el}} \ll E_s$.

the tensor depends on the polarization P_0 and on the external electric field E_{ext} . The dielectric tensor of the FE substrate is $\hat{\epsilon}^{\text{FE}} = 1 + \hat{\chi}^{\text{FE}}$. Finally, the FE substrate is characterized by the polarization $P_0(E_{\text{ext}})$ and the dielectric tensor $\hat{\epsilon}^{\text{FE}}$.

The sphere is located in the media with effective dielectric constant ϵ . Thus, we replace the layered structure above the FE substrate by the effective medium with homogeneous electric properties in our simplified model. We discuss the validity of this approach in Appendix Appendix C. For the Coulomb energy of the charged sphere we find [36, 37]

$$E_c = E_c^0 \frac{1}{\epsilon} \left(1 + \frac{a}{h} \frac{\epsilon - \epsilon^{\text{FE}}}{\epsilon + \epsilon^{\text{FE}}} \right), \quad (1)$$

where $E_c^0 = e^2/a$ is the Coulomb energy of the charged sphere in vacuum. Following the paper of Mele [37] we introduce an effective dielectric permittivity of the ferroelectric $\epsilon^{\text{FE}} = \sqrt{\hat{\epsilon}_{zz}^{\text{FE}} \hat{\epsilon}_{xx}^{\text{FE}}}$. The presence of FE substrate suppresses the Coulomb energy E_c due to the interaction of a charged grain with the image charge appearing inside the FE, figure 2(a). Equation (1) does not take into account the work of external field produced on the charge e assuming that electrons can move in the (x, y) -plane only.

4. Screened Coulomb interaction of two electrons

Second important parameter characterizing the properties of granular film is the screened Coulomb interaction of electrons located in different grains. We use the same model as in the previous section to find the influence of the FE substrate on the Coulomb interaction inside the granular film. The Coulomb interaction in layered system is considered in Appendix Appendix C. Consider two electrons at distances h_1 and h_2 above the FE surface and at distance l apart from each other in the (x, y) -plane. Electrons are located in the medium with effective dielectric constant ϵ and FE has the permittivity ϵ^{FE} . For interaction of two electrons we find [36]

$$U_c = U^0 \frac{1}{\epsilon} \left(1 + \frac{r_{12}}{r'_{12}} \frac{\epsilon - \epsilon^{\text{FE}}}{\epsilon + \epsilon^{\text{FE}}} \right), \quad (2)$$

where $r_{12} = \sqrt{l^2 + (h_1 - h_2)^2}$ is the distance between the electrons, $r'_{12} = \sqrt{l^2 + (h_1 + h_2)^2}$ is the distance between one of the electron and the image of the second electron inside the FE substrate, and $U^0 = e^2/r_{12}$ is the Coulomb interaction of electrons in vacuum.

5. Intergrain exchange interaction

Here we discuss the intergrain exchange interaction in the system shown in figure 1. We assume that all grains are in the FM state and that the grain magnetism is due to the itinerant (delocalized) electrons. This is valid for transition d-metals such as Ni, Co and Fe. The magnetic ordering in the whole system appears due to the intergrain exchange interaction J . We assume that exchange interaction between grains is also due

to the itinerant electrons. The wave functions of these electrons located in different grains overlap leading to the following exchange interaction [38],

$$J \propto \sum \int \Psi_1^*(\mathbf{r}_2) \Psi_2^*(\mathbf{r}_1) U_c(\mathbf{r}_1 - \mathbf{r}_2) \Psi_1(\mathbf{r}_1) \Psi_2(\mathbf{r}_2) d\mathbf{r}_1 d\mathbf{r}_2. \quad (3)$$

Here $\Psi_{1,2}$ is the spatial part of the electron wave function located in the first (second) grain; U_c is the Coulomb interaction of electrons located in different grains. Summation is over the different electron pairs in the grains.

We assume that the Coulomb gap, E_c , is large and that conduction electrons are localized inside grains. Outside the grains the electron wave functions exponentially decay

$$\Psi_{1,2}(\mathbf{r}) = A \begin{cases} e^{-\frac{a}{\xi}}, & |\mathbf{r} \pm \mathbf{r}_g/2| < a, \\ e^{-\frac{|\mathbf{r} \pm \mathbf{r}_g/2|}{\xi}}, & |\mathbf{r} \pm \mathbf{r}_g/2| > a. \end{cases} \quad (4)$$

Here $A = (\int |\Psi_{1,2}|^2 d\mathbf{r})^{-1/2}$ is the normalization constant and r_g is the distance between two grain centers. The electron localization length ξ in granular media depends on the Coulomb gap in the following way $\xi = a / \ln(E_c^2 / T^2 g_t)$, where g_t is the average intergrain conductance [34]. It was shown above that the Coulomb gap E_c and the Coulomb intergrain interaction U_c depend on the dielectric constant ϵ^{FE} of the FE substrate. Substituting (1), (2), and (4) into (3) we obtain the following result for the exchange integral

$$J \propto J_0 \epsilon^{\frac{4d}{a}-1} \left(1 + \frac{r_g}{r'_g} \frac{\epsilon - \epsilon^{\text{FE}}}{\epsilon + \epsilon^{\text{FE}}} \right)^{-\frac{4d}{a}} \left(1 + \frac{a}{h} \frac{\epsilon - \epsilon^{\text{FE}}}{\epsilon + \epsilon^{\text{FE}}} \right), \quad (5)$$

where $r'_g = \sqrt{r_g^2 + 4\hbar^2}$ and $d = r_g - 2a$. J_0 decays exponentially with increasing the intergrain distance d leading to the decrease of overall exchange coupling J in Eq. (5) with increasing the distance d . This is the consequence of the exponential decay of electron wave functions in the insulating matrix. Equation (5) shows that the FE substrate strongly influences the intergrain exchange interaction. The large factor $\frac{4d}{a}$ in the exchange integral J appears due to the high sensitivity of the exchange interaction to the ratio of intergrain distance d and the decay length of the wave function ξ . This ratio is defined by the Coulomb blockade effects which can be controlled by temperature and electric field. The sensitivity of exchange interaction on dielectric constant ϵ variations increases with decreasing grain size a , since the Coulomb blockade effects become more important in this case. The sensitivity of exchange interaction on dielectric constant ϵ variations increases with increasing the intergrain distance d . However, the overall exchange interaction decreases in this case. Increasing the granular film height h one decreases the coupling since the Coulomb interaction between grains and the FE layer decreases in this case.

The dielectric permittivity of FE, ϵ^{FE} , can be tuned by the external electric field or temperature, thus opening the possibility to control the exchange coupling constant.

6. Magnetic state of granular thin film

In this section we study the magnetic state of granular thin film using the mean field approximation (MFA) [39, 32, 31]. It is valid because the total grain spin is much larger than $\hbar/2$. We assume that all grains have the same magnetic moment μ with the total sample magnetization $M = y\mu$, where y is defined by the following equation

$$y = \coth\left(\frac{\mu B_{\text{ext}} + by}{T}\right) - \frac{T}{\mu B_{\text{ext}} + by}. \quad (6)$$

Here B_{ext} is the external magnetic field and $b = b(T)$ is the temperature dependent Weiss constant. It is related to the magnetic ordering temperature $T_m = b/3$ and to the microscopic exchange constant J , $b = zJ$, where z is the coordination number [39, 38]. Using (5) we find

$$b = b_0 \epsilon^{\frac{4d}{a}-1} \left(1 + \frac{r_g}{r'_g} \frac{\epsilon - \epsilon^{\text{FE}}}{\epsilon + \epsilon^{\text{FE}}}\right)^{-\frac{4d}{a}} \left(1 + \frac{a}{h} \frac{\epsilon - \epsilon^{\text{FE}}}{\epsilon + \epsilon^{\text{FE}}}\right), \quad (7)$$

where b_0 is the Weiss constant with dielectric constant $\epsilon = 1$.

Figure 3 shows the constant b vs. temperature T and external electric fields E_{ext} for granular film consisting of Ni grains with average radius $a = 2.5$ nm embedded into SiO_2 insulating matrix with the average intergrain distance $r_g \approx 1.3$ nm and with film effective dielectric constant $\epsilon_G = (a + r_g)\epsilon^{\text{SiO}_2}/(2r_g) \approx 6$, where $\epsilon^{\text{SiO}_2} \approx 4$ is the dielectric constant of SiO_2 . The effective dielectric constant of the upper halfspace in this case is $\epsilon \approx 5$. The constant b_0 is estimated using experimental data of Bozowski [31]. For Ni concentration 0.45% the FM state appears at temperature $T = 100\text{K}$.

We consider P(VDF/TrFE)(72/28) material for ferroelectric substrate. It has low dielectric constant ($\epsilon < 100$) and well pronounced polarization hysteresis loop [40, 41, 42]. We use the notation $\epsilon^{\text{FE}}(T, E_{\text{ext}})$ for dielectric constant. The distance between the granular film centre and the ferroelectric substrate is $h = 12$ nm. The behavior of dielectric permittivity vs. temperature and electric field is shown in Appendix Appendix A.

The straight dotted line in figure 3(a) stands for temperature T . The region with $b(T)/3 > T$ corresponds to the FM state of the granular film. Since the constant b has a maximum in the vicinity of FE phase transition point T_C^{FE} , the temperature line intersects $b(T)$ -curve twice leading to the existence of FM state in the temperature interval $T_C^{\text{L}} < T < T_C^{\text{H}}$.

The inverse phase transition occurs at temperature T_C^{L} with magnetic order appearing with increasing the temperature. Outside the FE region $[T_C^{\text{L}}, T_C^{\text{H}}]$ the granular film is in the superparamagnetic state. Figure 3 shows that the FM state occurs at much higher temperatures in comparison to granular Ni film without FE substrate [31], where magnetic phase transition appears at $T = 100\text{K}$. This is happening due to suppression of the Coulomb blockade in the vicinity of FE Curie temperature [43] and the increase of intergrain magnetic coupling. For temperatures $T < 100\text{K}$ the superparamagnetic-ferromagnetic phase transition appears [31].

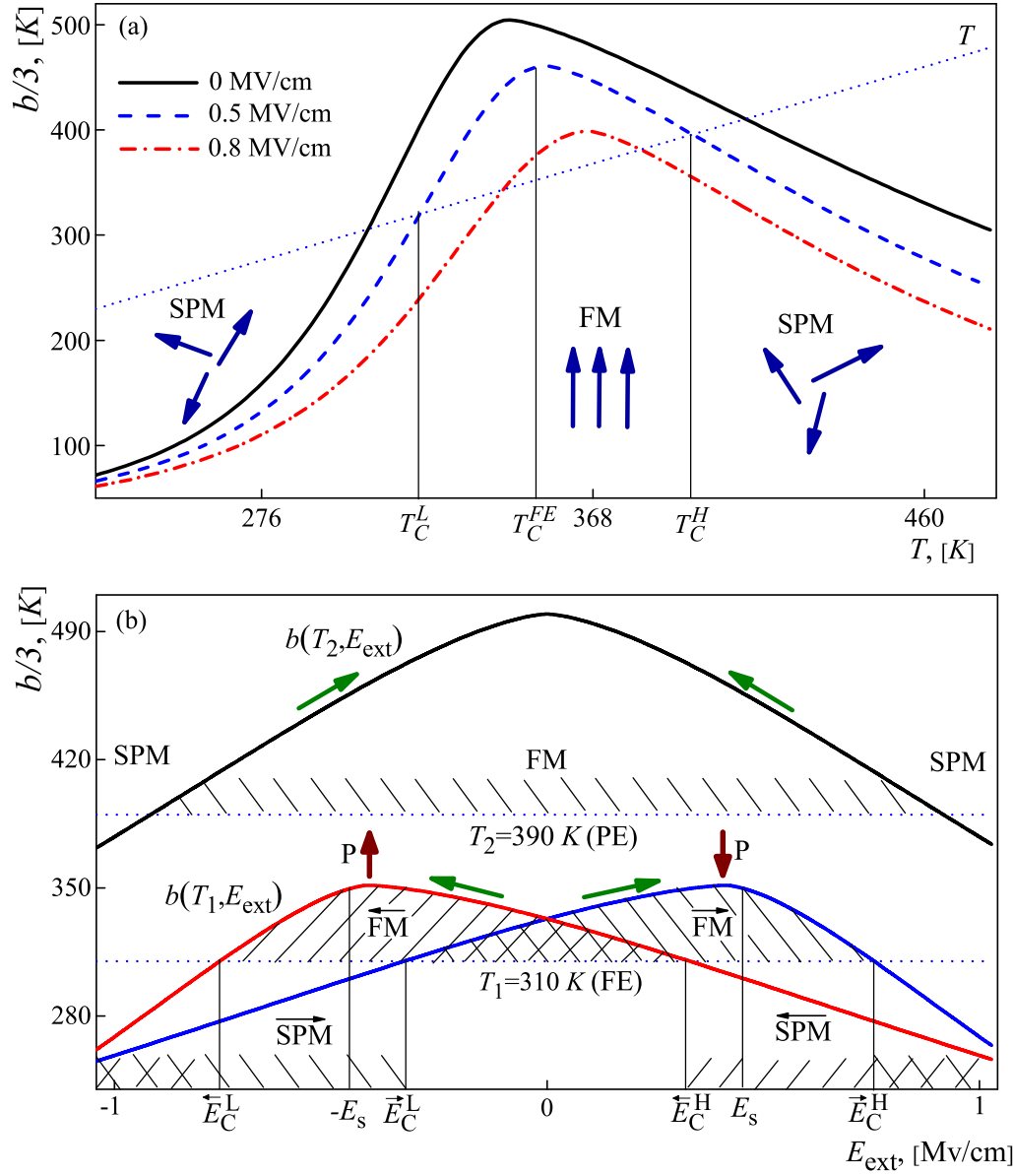


Figure 3. (Color online) (a) Weiss constant b , (7), vs. temperature for different external electric fields E_{ext} . The curves correspond to Ni granular thin film placed above P(VDF/TrFE) ferroelectric (FE) substrate. Dotted line stands for temperature T . Intersections of temperature and Weiss constant b curves correspond to the superparamagnetic-ferromagnetic (SPM-FM) phase transition. For temperatures $T_C^L < T < T_C^H$ the granular film is in the ferromagnetic (FM) state. Outside this region the film is in the SPM state. Transition temperatures T_C^L and T_C^H depend on the external electric field, E_{ext} . (b) Weiss constant b vs. external electric field E_{ext} for different temperatures. At high temperature, $T_2 = 390$ K the FE substrate is in the paraelectric (PE) state with zero spontaneous polarization of the substrate. At low external electric fields, $b(T, E_{\text{ext}}) > T$, the magnetic moments of granular film are ordered (FM state). At high electric fields, $b(T, E_{\text{ext}}) < T$, the magnetic film is in the SPM state. At low temperatures, $T_1 = 310$ K, the FE substrate has finite spontaneous polarization. The red up and down arrows show the direction of FE substrate polarization P . The green arrows indicate the path around the hysteresis loop. Critical fields \vec{E}_C^H and \vec{E}_C^L stand for electric field induced magnetic phase transitions for one branch and \vec{E}_C^L and \vec{E}_C^H for another branch.

The position of FE Curie temperature depends on the external electric field E_{ext} leading to the possibility of controlling the magnetic state of granular magnetic film by the external field. Figure 3(b) shows the dependence of the Weiss constant b on the external electric field E_{ext} . At temperatures $T > T_2 = 390$ K the FE substrate is in the paraelectric (PE) state with dielectric permittivity of the FE substrate monotonically decreasing with increasing the field E_{ext} . In the PE state the substrate has zero spontaneous polarization. According to (7) the magnetic coupling between grains decreases too. At low electric fields the granular film is in the FM state and at high fields it is in the SPM state. Thus, the electric field driven magnetic phase transition occurs in composite multiferroics.

At low temperatures the FE substrate is in the FE state with finite polarization P which can be switched by the external field E_{ext} . The switching field is $\pm E_s$. At these fields the dielectric permittivity of FE substrate and the intergrain exchange coupling have maxima. Due to the hysteresis behavior of dielectric constant the magnetic phase transition field depends on the branch. The fields \overleftarrow{E}_C^H and \overleftarrow{E}_C^L stand for electric field induced magnetic phase transition for one branch and \overrightarrow{E}_C^H and \overrightarrow{E}_C^L for another branch. For electric fields $\overleftarrow{E}_C^H < E_{\text{ext}} < \overrightarrow{E}_C^H$ and $\overleftarrow{E}_C^L < E_{\text{ext}} < \overrightarrow{E}_C^L$ the magnetic states are different for different branches. Thus, the magnetic state of granular film depends on the electric polarization P .

Substituting (7) into (6) we find the magnetization of composite multiferroics as a function of electric E_{ext} and magnetic B_{ext} fields and temperature T , figure 4. For zero magnetic field, $B_{\text{ext}} = 0$ the average magnetization M is finite for temperatures $T_C^L < T < T_C^H$ and it reaches its maximum at the point of maximum dielectric susceptibility of FE substrate, figure 4(a). The position of this maximum depends on the applied external electric field. For temperatures $T > T_C^{\text{FE}}$ the magnetization monotonically decreases with increasing the electric field up to the point where the granular film reaches the superparamagnetic state with zero average magnetic moment, figure 4(b). Below T_C^{FE} the magnetization is strongly depend on the substrate polarization P due to the hysteresis behavior of FE substrate. For negative polarization the increase of electric field E_{ext} ($E_{\text{ext}} < E_s$) leads to the increase of magnetization M , figure. 7. For positive polarization, increasing of electric field destroys the magnetic order. The external magnetic field B_{ext} smears the phase transition boundaries.

Figure 5 shows the magnetic susceptibility of granular film, $\chi_M = \partial M / \partial B_{\text{ext}}$, which can be controlled by the external electric field and which depends on the electric polarization of the FE substrate.

7. Phenomenological description of magneto-electric coupling

Here we discuss a phenomenological description of magneto-electric coupling in composite multiferroic system consisting of a granular FM film placed above the FE substrate, figure 1. The Weiss constant b has a quadratic dependence on external electric field E_{ext} for small fields and temperatures $T > T_C^{\text{FE}}$. For these parameters the

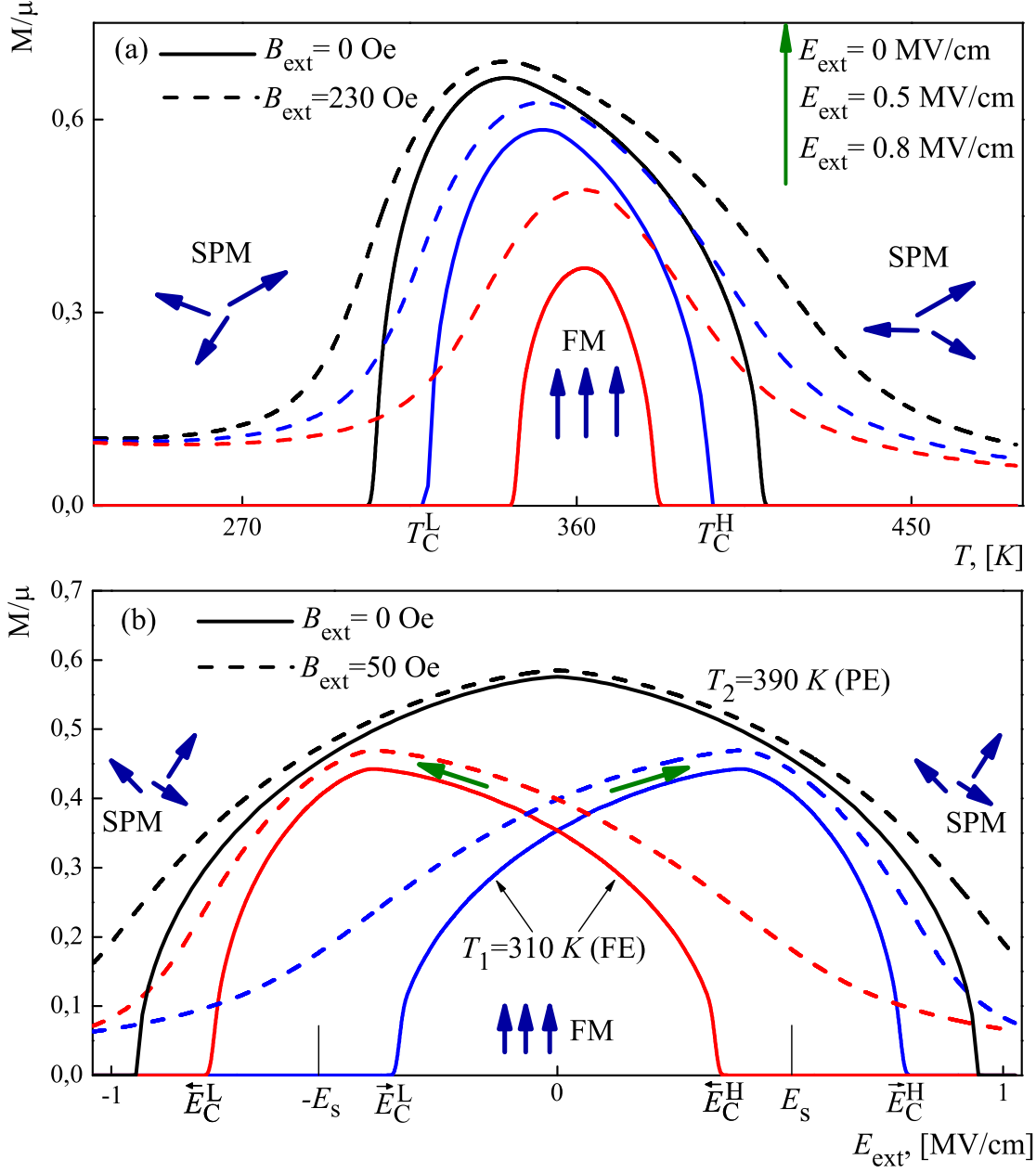


Figure 4. (Color online) (a) Dimensionless magnetization of granular film M/μ in (6) vs. temperature at different external electric and magnetic fields. The curves correspond to Ni granular thin film placed above P(VDF/TrFE) ferroelectric substrate. Regions of ordered (FM) and disordered (SPM) magnetic states correspond to those in Fig. 3(a). Magnetization decreases with increasing the electric field E_{ext} . (b) Dimensionless magnetization of granular film M/μ vs. external electric field E_{ext} at different temperatures and external magnetic fields B_{ext} . Curves correspond to the Weiss constant b shown in figure 3(b).

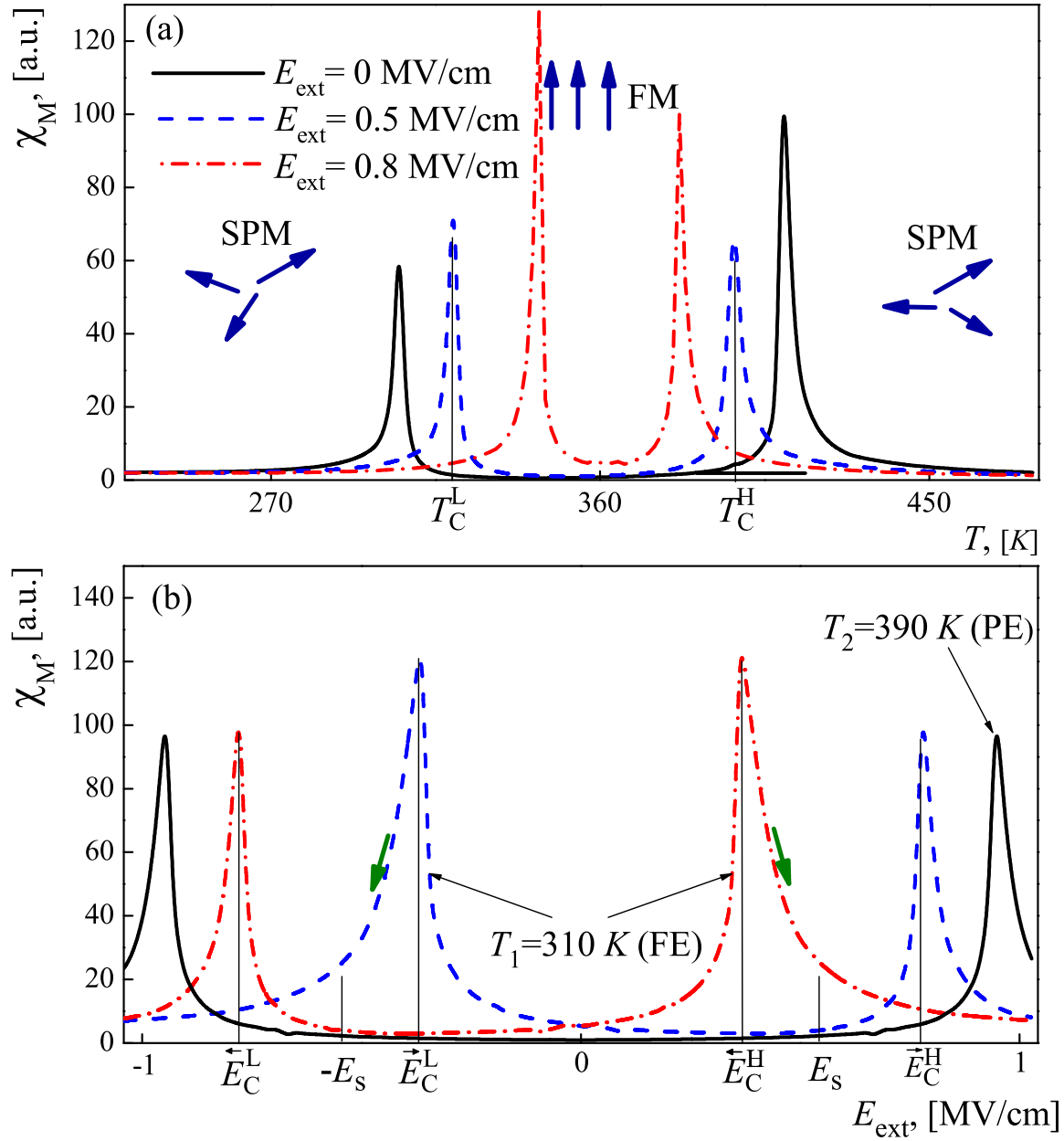


Figure 5. (Color online) (a) Magnetic susceptibility of granular film χ_M vs. temperature at different external electric fields. It has peaks in the vicinity of SPM-FM phase transitions. (b) Magnetic susceptibility χ_M vs. external electric field E_{ext} at different temperatures. The curves correspond to Ni granular thin film placed above P(VDF/TrFE) ferroelectric substrate.

electric polarization of the FE substrate P is linear in field E_{ext} leading to the quadratic dependence of the Weiss constant on polarization, $b \sim P^2$. In phenomenological approach the influence of electric polarization P on the Weiss constant b and on the FM ordering temperature T_M is described as follows $\gamma_{\text{me}}^1 M^2 P^2$, where γ_{me}^1 is some phenomenological parameter. For temperatures $T < T_{\text{C}}^{\text{FE}}$ the Weiss constant b depends on the mutual orientation of polarization and electric field, $\gamma_{\text{me}}^2 M^2 (\mathbf{P} \mathbf{E}_{\text{ext}})$. Thus, the total “magneto-electric energy” is

$$W_{\text{me}} = \gamma_{\text{me}}^1 M^2 P^2 + \gamma_{\text{me}}^2 M^2 (\mathbf{P} \mathbf{E}_{\text{ext}}). \quad (8)$$

It is important that the magneto-electric coupling in (8) is non-linear, quadratic, in contrast to the magneto-electric effects appearing due to the spin-orbit interaction [5].

8. Magneto-resistance of granular multiferroics

In this section we consider the magneto-resistance properties of composite multiferroics assuming that in addition to the external field E_{ext} there is a small voltage bias applied along the film producing a finite current. The conductivity of granular materials is defined by the following three factors [44, 34]: i) the suppression due to Coulomb blockade, $\sim e^{-E_c/T}$ with $E_c \gg T$, ii) the dependence of tunneling conductance on the mutual orientation of grain magnetic moments, and iii) the influence of exchange interaction on the Coulomb blockade. The conductivity is given by the following expression,

$$\sigma = \sigma_+^0 \frac{1 + \eta}{2} e^{-\frac{E_c + E_m}{T}} + \sigma_-^0 \frac{1 - \eta}{2} e^{-\frac{E_c - E_m}{T}}, \quad (9)$$

where η is the relative spin polarization of electrons in a single grain, $\eta = (n^\uparrow - n^\downarrow)/(n^\uparrow + n^\downarrow)$, with $n^{\uparrow\downarrow}$ being the numbers of electrons with spins “up” and “down”, $\sigma_\pm^0 = \sigma^0(1 \pm \zeta \langle M_i \cdot M_j \rangle / \mu^2)$ is the intergrain conductivity with σ^0 being the spin independent conductivity, and ζ being the small parameter describing the spin dependent tunneling [45]. The quantity E_m is the average difference of exchange energies inside different grains

$$E_m(T, B_{\text{ext}}, E_{\text{ext}}) = \frac{1}{2} J_{\text{int}} \cdot \left(1 - \frac{\langle M_i \cdot M_j \rangle}{\mu^2} \right), \quad (10)$$

with J_{int} being the exchange energy of electrons located in the same grain. Two energies J_{int} and J are different. The energy J is the exchange interaction of electrons located in different grains, it defines the ordering temperature T_m ; $J_{\text{int}} \gg J$. We introduce the notation for correlation function in (10), $C_m(T, B_{\text{ext}}, E_{\text{ext}}) = \langle M_i \cdot M_j \rangle / \mu^2$, [44]. In MFA it has the form $C_m(T, B_{\text{ext}}, E_{\text{ext}}) = y^2$.

Using (9) and the correlation function $C_m(T, B_{\text{ext}}, E_{\text{ext}})$ we find the magnitude of magneto-resistance effect,

$$\text{MR}(T, B_{\text{ext}}, E_{\text{ext}}) = \frac{\sigma(T, B_{\text{ext}}, E_{\text{ext}}) - \sigma(T, 0, E_{\text{ext}})}{\sigma(T, B_{\text{ext}}, E_{\text{ext}})}. \quad (11)$$

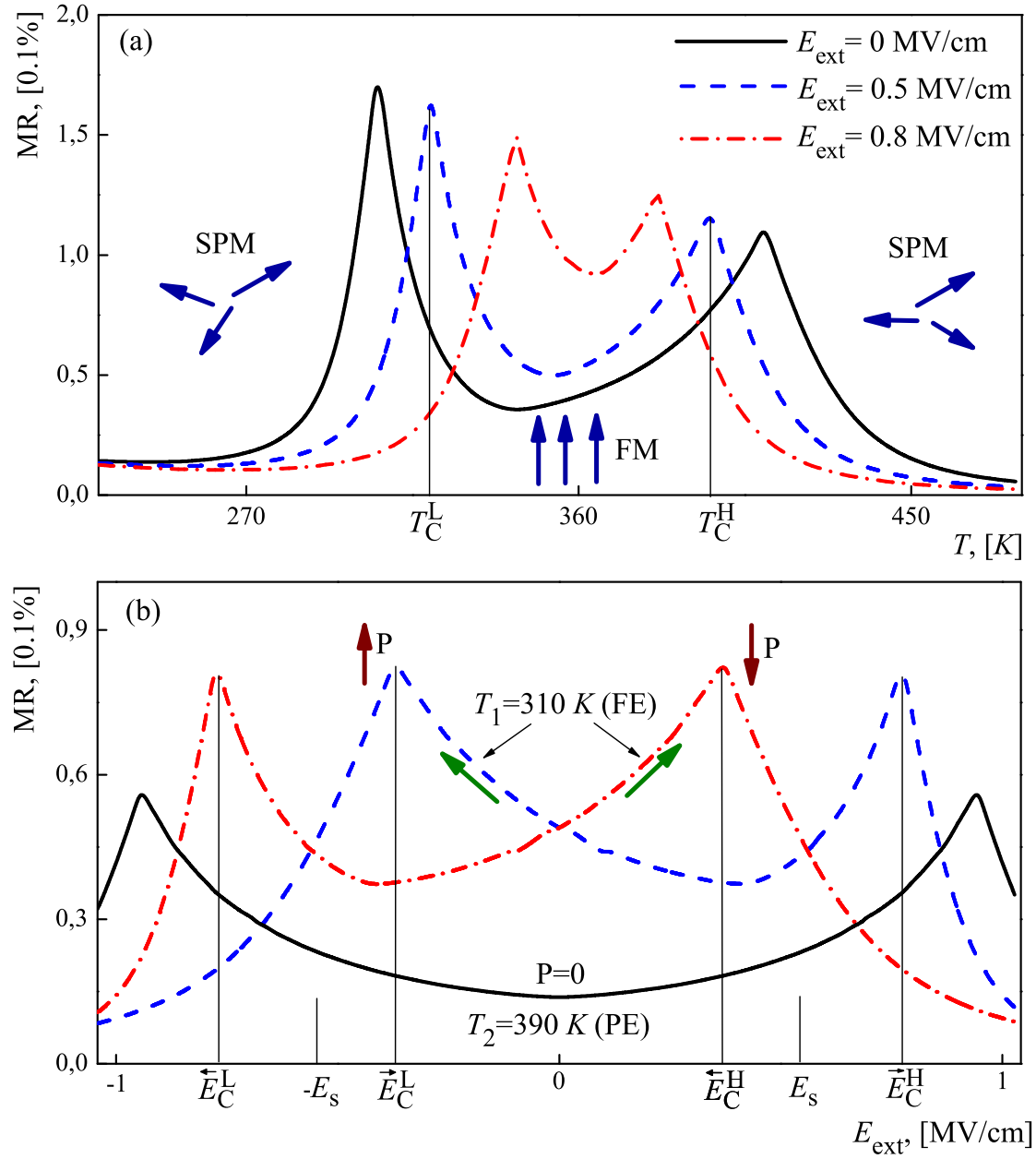


Figure 6. (Color online) (a) Magneto-resistance MR effect in composite multiferroic system, (11) and (12), vs. temperature at different external electric fields and fixed external magnetic field $B_{\text{ext}} = 200$ Oe. (b) MR effect in granular film vs. external electric field E_{ext} at different temperatures and fixed external magnetic fields $B_{\text{ext}} = 50$ Oe. All curves correspond to Ni granular thin film placed above P(VDF/TrFE) ferroelectric substrate.

For small electron polarization, $\zeta \ll 1$, $\eta \ll 1$ or small exchange constant J_{int} we find

$$\text{MR} \approx \eta \left(\zeta + \frac{J_{\text{int}}}{2T} \right) [C_m(T, B_{\text{ext}}, E_{\text{ext}}) - C_m(T, 0, E_{\text{ext}})]. \quad (12)$$

It follows from (12) that magneto-resistance effect is controlled by the expression $\eta\zeta + \eta J_{\text{int}}/2T$. Figure 6 shows the MR effect vs. temperature T and external electric field E_{ext} .

The temperature dependence of MR effect has two pronounced peaks in the vicinity of PE - FE phase transition in the FE substrate, figure 6(a). Each peak is associated with magnetic phase transition [31, 32] due to increase of magnetic fluctuations. In contrast to the materials with single magnetic Curie point, the composite multiferroics have two magnetic phase transitions in the vicinity of the FE Curie temperature leading to the occurrence of two MR peaks.

The positions of these peaks and their magnitude is controlled by the external electric field E_{ext} applied perpendicular to the system, figure 1. Figure 6(b) shows the MR effect vs. external electric field. For temperatures $T = 390 \text{ K} > T_{\text{C}}^{\text{FE}}$ the FE substrate is in the paraelectric state. In this case the MR effect has two maxima at certain fields $E_{\text{ext}} = \pm E_c$. These maxima appear at points of magnetic phase transition driven by the external electric field.

Below the FE phase transition, at temperatures $T = 310 \text{ K}$, the MR effect is more pronounced since the ratio $\eta J_{\text{int}}/2T$ becomes larger. The FE substrate and the MR effect demonstrate a hysteresis behavior. Arrows in figure 6 indicate the path around the hysteresis loop. Each branch has two MR maxima associated with magnetic phase transition driven by the electric field. Therefore the MR effect can be controlled by the electric field and it depends on the electric polarization of the substrate.

9. Conclusion

We studied magnetic and transport properties of multiferroic system consisting of granular ferromagnetic thin film placed above the FE substrate. We showed that magnetic state of the system strongly depends on temperature, external electric field, and electric polarization of the FE substrate. The FM state exists at finite temperature range around the FE phase transition point. Outside this region the superparamagnetic phase appears. Both the magnetic phase transition temperature and the magnitude of magnetization are strongly electric field dependent. In addition, the magnetic phase transition can be controlled by the external electric field. The magnetic state of the system depends on the mutual orientation of external electric field and polarization of FE substrate. The ferromagnetic and ferroelectric degrees of freedom are coupled due to the influence of FE substrate on the screening of intragrain and intergrain Coulomb interaction.

Also we studied the conductivity of composite multiferroic system and showed that MR effect strongly depends on temperature, external electric field, and electric polarization of the FE substrate. The MR effect has two maxima related to two magnetic

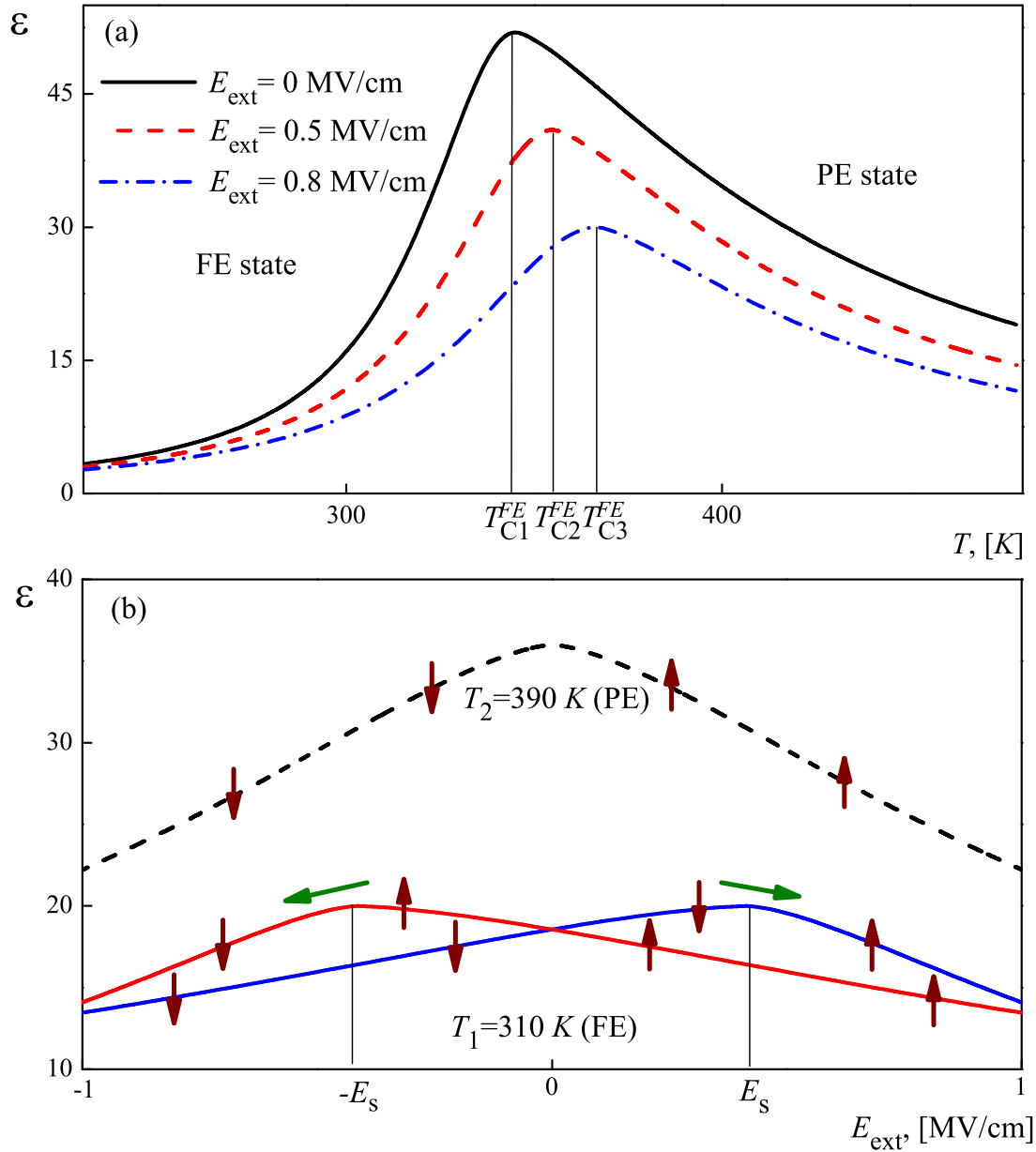


Figure 7. (Color online) (a) Dielectric permittivity vs. temperature at different external electric fields E_{ext} . $T_{C1,2,3}^{\text{FE}}$ stand for temperatures of paraelectric-ferroelectric (PE - FE) phase transition. (b) Dielectric permittivity vs. external electric field E_{ext} at different temperatures. Up and down arrows indicate the direction of average polarization P of the ferroelectric substrate. At temperature $T = 390$ K the polarization P has one component induced by the external electric field E_{ext} . At $T = 310$ K the polarization P has spontaneous and electric field induced components. Hysteresis loop exists at temperature $T = 310$ K. Horizontal arrows indicate the path around the hysteresis loop. $\pm E_s$ is the switching field of spontaneous polarization. At these points the dielectric permittivity reaches its maximum.

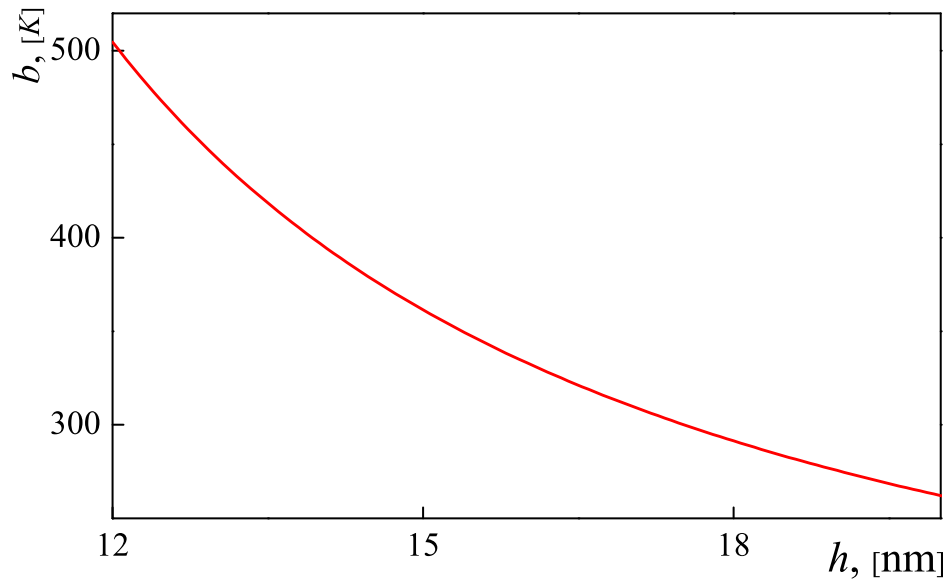


Figure 8. (Color online) Weiss constant b vs. distance h above the substrate.

phase transitions occurring in the vicinity of FE phase transition. The positions of these maxima can be shifted by the external electric field. The magnitude of MR effect depends on the mutual orientation of external electric field and polarization of the FE substrate.

We demonstrated that magnetic state and MR effect can be controlled by the electric field for some systems including Ni granular thin film placed above the FE substrate.

10. Acknowledgments

We thank Michael Huth for providing us with his manuscript prior publication. I. B. was supported by NSF under Cooperative Agreement Award EEC-1160504 and NSF Award DMR-1158666. N. C. was partly supported by RFBR No. 13-02-00579, the Grant of President of Russian Federation for support of Leading Scientific Schools, RAS presidium and Russian Federal Government programs.

Appendix A. Dielectric permittivity vs. temperature and electric field

Here we discuss the behavior of substrate dielectric permittivity as a function of temperature and external electric field. We estimate the dielectric permittivity of P(VDF/TrFE)(72/28) material using data of paper [40]. We use some smooth function to show the important features of $\epsilon(T)$ and $\epsilon(E_{\text{ext}})$ curves presented in paper [40]. The dielectric permittivity of P(VDF/TrFE)(72/28) has temperature hysteresis. In this

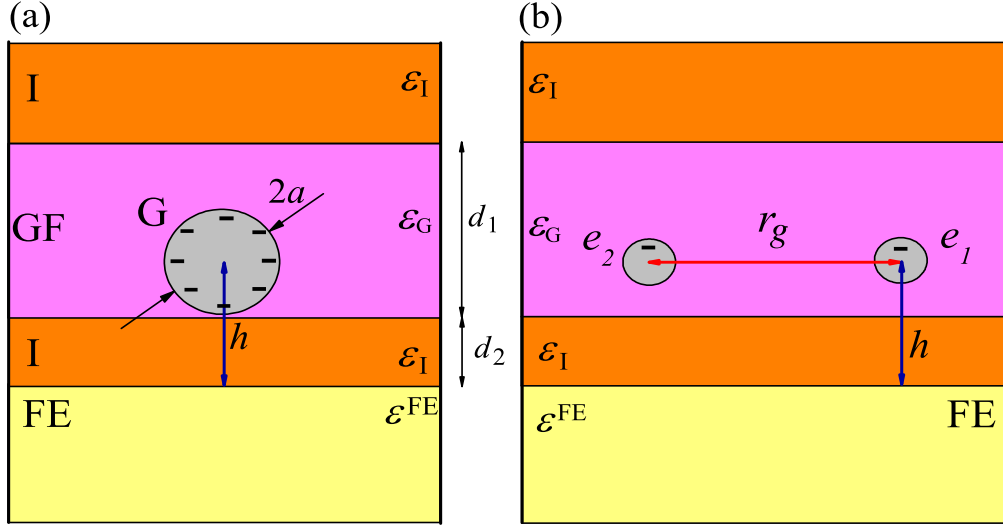


Figure A1. (Color online) Multilayer system consisting of FE substrate (FE) with dielectric constant ϵ^{FE} , insulating layers (I) with dielectric constants ϵ_I and granular film (GF). (a) Metallic grain (G) of size $2a$ is located above the FE substrate at distance h . Space around the grain in granular film is considered as an effective medium with dielectric constant ϵ_G . Granular film and the middle insulating layer have thickness d_1 and d_2 , respectively. (b) Two charges ($e_{1,2}$) at distance h above the FE substrate and distance r_g apart inside the granular film.

paper we consider only the “cooling” branch for simplicity. The dependencies $\epsilon(T)$ and $\epsilon(E_{\text{ext}})$ are shown in figure 7.

Appendix B. Exchange constant J vs. film thickness

In this appendix we discuss the dependence of exchange constant J on film thickness. For exchange J in (5) we assumed that all grains have the same distance above the FE substrate. This approximation is valid for thin films with just one layer of grains. For thick granular films the influence of FE substrate is different for layers located at different distance from the substrate. However, the dependence of exchange interaction J on grain positions is rather weak, (5) and figure 8. Therefore the influence of film thickness is not important. In addition, the exchange interaction J is exponentially depend on the intergrain distance r_g leading to a wide distribution of J for different pair of grains. Averaging over the distance r_g is assumed in our calculations eliminating the dependence of J on the distance from the substrate.

Appendix C. Charging energy of metallic grain in a layered system

The charging energy of metallic grain placed in a system consisting of several insulating layers (see figure A1) can be estimated as $E_c = e^2/(2C)$ with C being

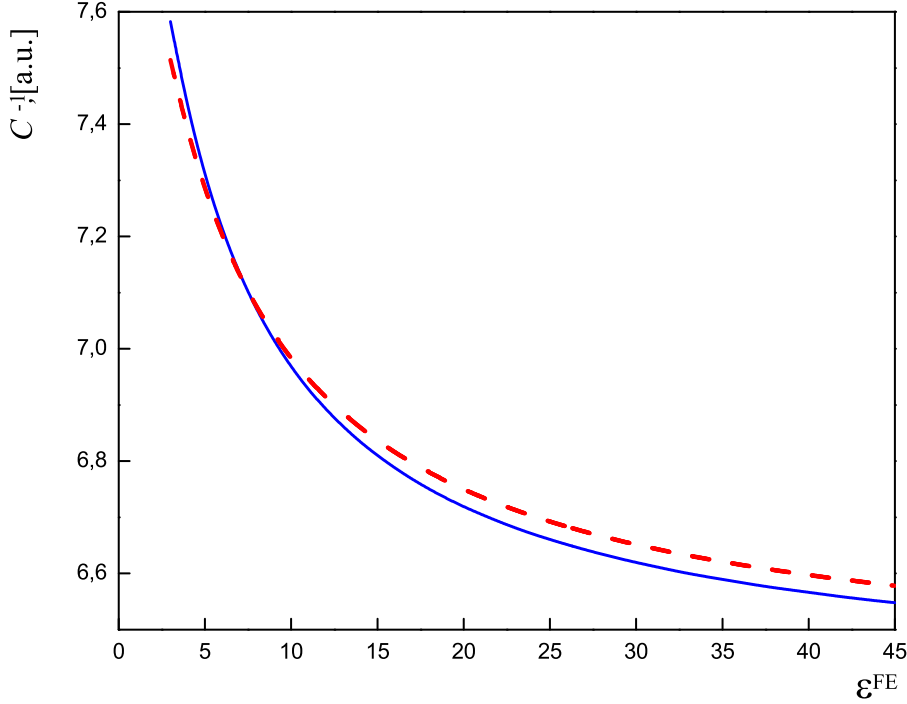


Figure C1. (Color online) Inverse capacitance C^{-1} of a metallic grain in layered system shown in figure A1 as a function of dielectric permittivity of FE substrate (perpendicular to the surface component of tensor $\hat{\epsilon}^{\text{FE}}$). Solid line corresponds to the numerical calculations for the layered system, (C.1). Dashed line stands for calculations with simplified system where upper halfspace being considered as homogeneous with effective dielectric permittivity ϵ , (1).

the grain capacitance. To find the capacitance C we use the source point collocation method. [46, 47] We consider the sphere as the ensemble of point charges q_i placed in the positions \mathbf{r}_i . We find charges q_i self-consistently assuming that all the points \mathbf{r}_i have the same potential $\phi_i = \phi$ and the total charge of the sphere is $Q = \sum q_i$. The potential at points \mathbf{r}_i can be found as

$$\phi_i = \phi = \sum q_j G_{ij}, \quad (\text{C.1})$$

where G_{ij} is the electric potential created at point \mathbf{r}_i by the unit charge located at point \mathbf{r}_j . The Green functions G_{ij} for layered system can be found using the two dimensional Fourier transformation. The capacitance $C = Q/\phi$ can be calculated after solving C.1.

We calculate the capacitance C as a function of dielectric permittivity ϵ^{FE} of the FE substrate for the following system: the granular film with 5 nm Ni grains embedded into SiO_2 matrix is placed above the P(VDF/TrFE) at distance 12 nm. The intergrain distance is 1.5 nm. The thickness of the film is 10 nm and the effective dielectric permittivity $\epsilon_{\text{G}} \approx 5$. We consider SiO_2 insulator with dielectric permittivity $\epsilon_{\text{I}} = 4$ placed above the granular film and in between the FE substrate and the granular film. The inverse capacitance C^{-1} vs. dielectric permittivity of the FE substrate is

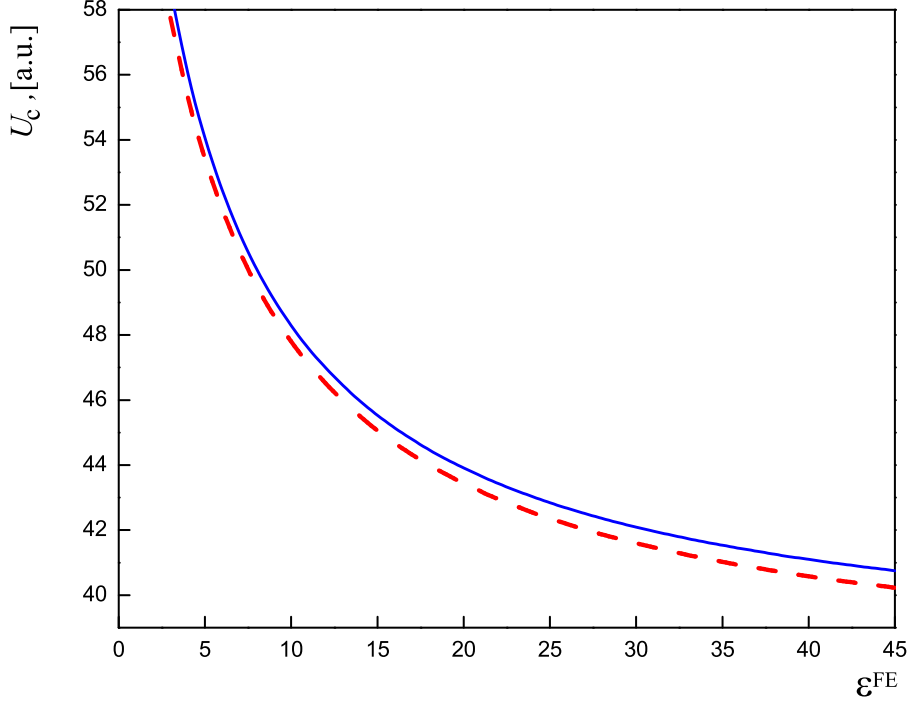


Figure C2. (Color online) Coulomb interaction U_c of two charges in layered system shown in figure A1 as a function of dielectric permittivity of the FE substrate. Solid line corresponds to numerical calculations for the layered system. Dashed line stands for U_c calculated using the simplified system with upper halfspace being considered as homogeneous with effective dielectric permittivity ϵ , (2).

shown in figure C1. The dotted line in figure C1 stands for the inverse capacitance behavior calculated using (1) with the effective dielectric permittivity $\epsilon = 4.5$. The numerical calculations with more complicated model produce almost the same result as the simplified model.

Appendix D. Coulomb interaction of two point charges in a layered system

Here we calculate the Coulomb interaction U_c vs. dielectric permittivity of the FE substrate in layered system (see figure C2). In figure C2 the distance between charges is 8 nm and the distance between charges and the FE is 12 nm. The geometrical parameters of the layered system are the same as in the previous subsection. The dashed line in figure C2 shows the U_c calculated using (2) with $\epsilon = 4.5$. The simplified model produces almost the same result as the more complicated model.

References

- [1] J. T. Heron, J. L. Bosse, Q. He, Y. Gao, M. Trassin, L. Ye, J. D. Clarkson, C. Wang, Jian Liu, S. Salahuddin, D. C. Ralph, D. G. Schlom, J. Iniguez, B. D. Huey, and R. Ramesh. *Nature*,

- 516:370, 2014.
- [2] T. Aoyama, K. Yamauchi, A. Iyama, S. Picozzi, K. Shimizu, and T. Kimura. *Nature Comm.*, 5:4927, 2014.
- [3] Kathrin Dorr and Andreas Herklotz. *Nature*, 516:337, 2014.
- [4] Wei-Gang Wang, Mingen Li, Stephen Hageman, and C. L. Chien. *Nature Mat.*, 11:64, 2012.
- [5] W. Eerenstein, N. D. Mathur, and J. F. Scott. *Nature*, 442:759, 2006.
- [6] R. Ramesh and Nicola A. Spaldin. *Nature Mat.*, 6:21, 2007.
- [7] Manuel Bibes and Agnes Barthelemy. *Nature Mat.*, 7:425, 2008.
- [8] D. Chiba, M. Sawicki, Y. Nishitani, Y. Nakatani, F. Matsukura, and H. Ohno. *Nature (London)*, 455:515, 2008.
- [9] M. Weisheit, S. Fahler, A. Marty, Y. Souche, C. Poinsignon, and D. Givord. *Science*, 315:349, 2007.
- [10] Masahito Tsujikawa and Tatsuki Oda. *Phys. Rev. Lett.*, 102:247203, 2009.
- [11] Chun-Gang Duan, Julian P. Velev, R. F. Sabirianov, Ziqiang Zhu, Junhao Chu, S. S. Jaswal, and E. Y. Tsymbal. *Phys. Rev. Lett.*, 101:137201, 2008.
- [12] H. Katsura, N. Nagaosa, and A. V. Balatsky. *Phys. Rev. Lett.*, 95:057205, 2005.
- [13] I. A. Sergienko and E. Dagotto. *Phys. Rev. B*, 73:094434, 2006.
- [14] Ce-Wen Nan. *Phys. Rev. B*, 50:6082, 1994.
- [15] C. Thiele, K. Dorr, O. Bilani, J. Rodel, and L. Schultz. *Phys. Rev. B*, 75:054408, 2007.
- [16] S. Geprags, A. Brandlmaier, M. Opel, R. Gross, and S. T. B. Goennenwein. *Appl. Phys. Lett.*, 96:142509, 2010.
- [17] S. M. Wu, Shane A. Cybart, D. Yi, James M. Parker, R. Ramesh, and R. C. Dynes. *Phys. Rev. Lett.*, 110:067202, 2013.
- [18] V. Laukhin, V. Skumryev, X. Marti, D. Hrabovsky, F. Sanchez, M. V. Garcia-Cuenca, C. Ferrater, M. Varela, U. Liders, J. F. Bobo, and J. Fontcuberta. *Phys. Rev. Lett.*, 97:227201, 2006.
- [19] Xi He, Yi Wang, Ning Wu, Anthony N. Caruso, Elio Vescovo, Kirill D. Belashchenko, Peter A. Dowben, and Christian Binek. *Nature Mat.*, 9:579, 2010.
- [20] M. Ye. Zhuravlev, S. Maekawa, and E. Y. Tsymbal. *Phys. Rev. B*, 81:104419, 2010.
- [21] V. Garcia, M. Bibes, L. Bocher, S. Valencia, F. Kronast, A. Crassous, X. Moya, S. Enouz-Vedrenne, A. Gloter, D. Imhoff, C. Deranlot, N. D. Mathur, S. Fusil, K. Bouzehouane, and A. Barthelemy. *Science*, 327:1106, 2010.
- [22] Chenglong Jia and Jamal Berakdar. *Phys. Rev. B*, 80:014432, 2009.
- [23] Chenglong Jia and Jamal Berakdar. *Phys. Rev. B*, 83:045309, 2011.
- [24] O. G. Udalov, N. M. Chtchelkatchev, and I. S. Beloborodov. *Phys. Rev. B*, 89:174203, 2014.
- [25] R. Ranjith, R. Nikhil, and S. B. Krupanidhi. *Phys. Rev. B*, 74:184104, 2006.
- [26] D. Bolten, U. Buttger, and R. Waser. *J. Appl. Phys.*, 93(3):1735, 2006.
- [27] Chen Ang and Zhi Yu. *Phys. Rev. B*, 69:174109, 2004.
- [28] Paolo Allia, Marco Coisson, Marcelo Knobel, Paola Tiberto, and Franco Vinai. *Phys. Rev. B*, 60:12207, 1999.
- [29] D. Kechrakos and K. N. Trohidou. *Phys. Rev. B*, 58:12169, 1998.
- [30] C. Bean and J. D. Livingston. *J. Appl. Phys.*, 30:120S, 1959.
- [31] J. I. Gittleman, Y. Goldstein, and S. Bozowski. *Phys. Rev. B*, 5:3609, 1972.
- [32] S. Barzilai, Y. Goldstein, I. Balberg, and J. S. Helman. *Phys. Rev. B*, 23:1809, 1981.
- [33] Ping Sheng, B. Abeles, and Y. Arie. *Phys. Rev. Lett.*, 31:44, 1973.
- [34] I. S. Beloborodov, A. V. Lopatin, V. M. Vinokur, and K. B. Efetov. *Rev. Mod. Phys.*, 79:469, 2007.
- [35] O. G. Udalov, N. M. Chtchelkatchev, and I. S. Beloborodov. *Phys. Rev. B*, 90:054201, 2014.
- [36] L. D. Landau and E. M. Lifshitz. *Course of Theoretical Physics: Vol.: 8: Electrodynamics of Continuous Media*. Pergamon Press, 1960.
- [37] E. J. Mele. *Am. Jour. Phys.*, 69:557, 2001.
- [38] A. Auerbach. *Interacting electrons and quantum magnetism*. Springer, 1994.

- [39] S. V. Vonsovskii. *Magnetism*. Wiley, New York, 1974.
- [40] Jong Soon Lee, Arun Anand Prabu, Kap Jin Kim, and Cheolmin Park. *Fibers and Polymers*, 8(5):456, 2007.
- [41] Kuniko Kimura and Hiroji Ohgashi. *Appl. Phys. Lett.*, 43:834, 1983.
- [42] Takeshi Yamada and Toyoki Kitayama. *J. Appl. Phys.*, 52:6859, 1981.
- [43] O. G. Udalov, N. M. Chtchelkatchev, A. Glatz, and I. S. Beloborodov. *Phys. Rev. B*, 89:054203, 2014.
- [44] J. S. Helman and B. Abeles. *Phys. Rev. Lett.*, 37:1429, 1976.
- [45] I. S. Beloborodov, A. Glatz, and V. M. Vinokur. *Phys. Rev. Lett.*, 99:066602, 2007.
- [46] M. Huth, F. Kolb, and H. Plank. *Appl. Phys. A*, (to be published), 2014.
- [47] C. Wasshuber. *Computational Single-Electronics*. Springer, Wien/New York, 2001.